JASN

Adiponectin Promotes Monocyte-to-Fibroblast Transition in Renal Fibrosis

Jun Yang,[*][†] Song-Chang Lin,[*] Gang Chen,[*][‡] Liqun He,[‡] Zhaoyong Hu,[*] Lawrence Chan,[§] JoAnn Trial,[‖] Mark L. Entman,[‖] and Yanlin Wang[⊠][*]

[*]Division of Nephrology and

[§]Division of Endocrinology and Metabolism, Department of Medicine, Baylor College of Medicine, Houston, Texas;

[†]Department of Urology, Union Hospital, Tongji Medical College, Huazhong University of Science and Technology, Wuhan, Hubei, China;

[‡]Division of Nephrology, Department of Medicine, Shuguang Hospital, Shanghai, China; and

[‖]Division of Cardiovascular Sciences and the DeBakey Heart Center, Department of Medicine, Baylor College of Medicine and The Methodist Hospital, Houston, Texas

[⊠]Corresponding author.

Correspondence: Dr. Yanlin Wang, Department of Medicine-Nephrology, Baylor College of Medicine, BCM395, One Baylor Plaza, Houston TX 77030., Email: yanlinw@bcm.edu

Abstract

Bone marrow–derived fibroblasts may contribute substantially to the pathogenesis of renal fibrosis through the excessive production and deposition of extracellular matrix. However, the mechanisms underlying the accumulation and activation of these fibroblasts are not understood. Here, we used a mouse model of tubulointerstitial fibrosis to determine whether adiponectin, which is elevated in CKD and is associated with disease progression, regulates monocyte-to-fibroblast transition and fibroblast activation in injured kidneys. In wild-type mice, the expression of adiponectin and the number of bone marrow–derived fibroblasts in the kidney increased after renal obstruction. In contrast, the obstructed kidneys of adiponectin-knockout mice had fewer bone marrow–derived fibroblasts. Adiponectin deficiency also led to a reduction in the number of myofibroblasts, the expression of profibrotic chemokines and cytokines, and the number of procollagen-expressing M2 macrophages in injured kidneys. Consistent with these findings, adiponectin-deficiency reduced the expression of collagen I and fibronectin. Similar results were observed in wild-type and adiponectin-knockout mice after ischemia-reperfusion injury. In cultured bone marrow–derived monocytes, adiponectin stimulated the expression of α-smooth muscle actin (SMA) and extracellular matrix proteins and activated AMP-activated protein kinase (AMPK) in a time- and dose-dependent manner. Furthermore, specific activation of AMPK increased the expression of α-SMA and extracellular matrix proteins, while inhibition of AMPK attenuated these responses. Taken together, these findings identify adiponectin as a critical regulator of monocyte-to-fibroblast transition and renal fibrosis, suggesting that inhibition of adiponectin/AMPK signaling may represent a novel therapeutic target for fibrotic kidney disease.

Renal fibrosis is a final common manifestation of chronic kidney disease.[1,2] Renal interstitial fibrosis is characterized by fibroblast activation and excessive production and deposition of extracellular matrix (ECM), which leads to the destruction and collapse of renal parenchyma and progressive loss of kidney function. Because fibroblasts are the principal effector cells responsible for ECM production, their

activation is regarded as a key event in the pathogenesis of renal fibrosis.[3–5] However, the origin of these fibroblasts remains controversial. They are traditionally thought to arise from resident renal fibroblasts. Recent evidence indicates that they may originate from bone marrow–derived fibroblast progenitor cells.[6–10]

Bone marrow–derived fibroblast precursors or fibrocytes are derived from a subpopulation of monocytes *via* monocyte-to-fibroblast transition.[11–14] These cells express mesenchymal markers, such as collagen I and vimentin, and hematopoietic markers, such as CD45 and CD11b.[11,15–17] These cells in culture display an adherent, spindle-shape morphology and express α-SMA that is enhanced when cells are treated with TGF-β1, consistent with the concept that they can differentiate into myofibroblasts.[15–17] The differentiation of these cells is regulated by cytokines. Profibrotic cytokines—IL-4 and IL-13—promote myeloid fibroblast differentiation, whereas antifibrotic cytokines—IFN-γ and IL-12—inhibit its differentiation.[13,18] We and others have shown that these cells are involved in the pathogenesis of renal fibrosis.[4,7,12] However, the molecular mechanisms underlying the recruitment and maturation of these cells in injured kidneys are not fully understood.

Adiponectin is a multifunctional cytokine that plays an important role in the regulation of energy metabolism and inflammation.[19,20] It was initially reported to be synthesized exclusively by adipocytes.[21] However, recent studies have shown that it is also produced by other cell types, such as endothelial cells,[22] inflammatory cells,[22,23] and epithelial cells.[24,25] Circulating adiponectin levels are elevated in patients with chronic kidney disease, and a high level of adiponectin is associated with increased overall and cardiovascular mortality and progression of chronic kidney disease.[26,27] However, its role in renal fibrosis is not known.

In this study, we investigate the role of adiponectin in the activation of bone marrow–derived fibroblast precursors in the kidney in a well-established model of tubulointerstitial fibrosis induced by unilateral ureteral obstruction (UUO) and cultured bone marrow–derived monocytes. Genetic ablation or pharmacologic inhibition of adiponectin signaling inhibits monocyte-to-fibroblast transition and attenuates the development of renal interstitial fibrosis. These results establish a critical role of adiponectin signaling in monocyte-to-fibroblast transition and the pathogenesis of renal fibrosis.

RESULTS

Adiponectin Is Induced in a Mouse Model of Renal Fibrosis

We first characterized the induction of adiponectin in the kidney in a mouse model of tubulointerstitial fibrosis induced by UUO. Using real time RT-PCR, we found that the mRNA level of adiponectin was upregulated in injured kidneys compared with that of control kidneys after 5 days of UUO (Figure 1A). To identify the cell types responsible for adiponectin production in the kidney, serial sections of kidneys were stained with an antiadiponectin antibody. Our results revealed that adiponectin protein was localized mainly in the interstitial cells of obstructed kidneys (Figure 1B). Consistent with the immunohistochemical findings, Western blot analysis demonstrated that the protein levels of adiponectin were elevated in obstructed kidneys of wild-type (WT) mice compared with control kidneys (Figure 1, C and D).

Adiponectin Deficiency Impairs Myeloid Fibroblast Accumulation

To examine whether adiponectin plays a role in the accumulation of bone marrow–derived fibroblasts in the obstructed kidneys, WT and adiponectin-knockout (KO) mice were subjected to obstructive injury. Kidney sections were stained for CD45, a leukocyte maker, and platelet-derived growth factor receptor (PDGFR)-β, a mesenchymal marker. Our results revealed that the number of CD45^{+} and PDGFR-β^{+} cells was markedly increased in injured kidneys of WT mice, whereas the number of CD45^{+} and PDGFR-β^{+}

cells was significantly reduced in injured kidneys of adiponectin-KO mice (Figure 2, A and B). To further quantify the number of myeloid fibroblasts in the kidney, freshly dispersed kidney cells were stained for CD45 and collagen I and examined by flow cytometry. Our results showed that the number of CD45$^+$ and collagen I$^+$ fibroblasts was markedly increased in injured kidneys of WT mice, whereas the number of CD45$^+$ and collagen I$^+$ fibroblasts was significantly reduced in injured kidneys of adiponectin-KO mice (Figure 2, C and D). These data indicate that adiponectin plays a critical role in the accumulation of bone marrow–derived fibroblasts into the kidney.

Adiponectin Deficiency Inhibits Myofibroblast Formation

To determine whether adiponectin deficiency influences the development of bone marrow–derived myofibroblasts in the kidney, WT and adiponectin KO mice were subjected to UUO for 7 days. Kidney sections were stained for α-smooth muscle actin (SMA) and examined with a fluorescence microscope. Our results revealed that targeted deletion of adiponectin resulted in a significant reduction in the number of α-SMA$^+$ myofibroblasts in obstructed kidneys compared with those of WT mice (Figure 3, A and B). Consistent with these findings, Western blot analysis showed that adiponectin deficiency significantly reduced the protein expression level of α-SMA in obstructed kidneys compared with WT mice (Figure 3, C and D). These results indicate that adiponectin plays an important role in the activation and differentiation of bone marrow–derived fibroblasts.

Adiponectin Deficiency Attenuates Profibrotic Chemokine and Cytokine Production and M2 Macrophage Polarization

To elucidate the mediators that might be required for the reduction in CD45$^+$ myeloid fibroblasts in adiponectin KO mice, we investigated the effect of adiponectin deficiency on profibrotic chemokine and cytokine expression in the kidney. In our previous studies, we demonstrated that the appearance of myeloid fibroblasts was associated with monocyte chemotactic protein-1 (MCP-1) and CXCL16 induction.[10,28] Thus, we examined the mRNA levels of MCP-1 and CXCL16 in the kidney of WT and adiponectin KO mice. Our results showed that adiponectin deficiency reduced the mRNA expression of MCP-1 and CXCL16 (Figure 4A), indicating that these chemokines contribute to accumulation of myeloid fibroblasts in the kidney. Th2 cytokines, IL-4 and IL-13, have been shown to promote M2 macrophage polarization and monocyte to fibroblast transition,[13,18,29,30] and so we measured the effect of adiponectin deficiency on the production of IL-4 and IL-13 in the kidney. The mRNA levels of IL-13 and IL-4 were markedly increased in obstructed kidneys of WT mice, whereas the increase in the mRNA levels of IL-13 and IL-4 was significantly reduced in obstructed kidneys of adiponectin KO mice (Figure 4B). These data indicate that adiponectin may promote myeloid fibroblast accumulation and M2 macrophage polarization through chemokines and Th2 cytokines.

We next determined whether adiponectin deficiency affected macrophage polarization and myeloid fibroblast formation by subjecting WT and adiponectin KO mice to UUO for 7 days. The mRNA levels of CD206, a marker for M2 macrophages, were markedly increased in obstructed kidneys of WT mice, whereas the increase in CD206 mRNA was significantly reduced in obstructed kidneys of adiponectin KO mice (Figure 4C). These data indicate that adiponectin promotes M2 macrophage polarization. To determine whether M2 macrophages produce collagen, kidney sections were stained for CD206 and procollagen I. Our results revealed that the number of CD206 and procollagen I dual-positive cells was increased in obstructed kidneys of WT mice, whereas the number of CD206 and procollagen I dual-positive cells was significantly reduced in obstructed kidneys of adiponectin KO mice (Figure 4, D and E). These results support our hypothesis that myeloid fibroblasts are derived from monocytes through M2 macrophage polarization.

Adiponectin Deficiency Suppresses Renal Fibrosis

Because adiponectin regulates the accumulation of bone marrow–derived fibroblasts in the kidney in response to obstructive injury, we then examined the effect of adiponectin deficiency on the development of renal fibrosis. WT and adiponectin KO mice were subjected to UUO for 14 days. WT mice developed significant collagen deposition in obstructed kidneys, as demonstrated by picrosirius red staining, whereas these responses were significantly attenuated in obstructed kidneys of adiponectin KO mice (Figure 5, A and B). These data indicate that adiponectin plays a critical role in the pathogenesis of renal fibrosis.

We next investigated the effect of targeted disruption of adiponectin on the expression and accumulation of collagen I and fibronectin, two major components of ECM. The protein expression levels of collagen I and fibronectin increased markedly in obstructed kidneys of WT mice, whereas targeted deletion of adiponectin significantly suppressed the protein expression levels of these matrix proteins in obstructed kidneys (Figure 6, A–E). These data indicate that targeted deletion of adiponectin attenuates renal fibrosis by inhibiting production and deposition of ECM proteins.

Adiponectin Deficiency Suppresses Myeloid Fibroblast Accumulation and Renal Fibrosis after Ischemia-Reperfusion Injury

We have shown that adiponectin plays an essential role in the accumulation of CD45^{+} myeloid fibroblasts in the kidney in response to obstructive injury. We next determined if adiponectin regulates myeloid fibroblast accumulation and fibrosis development in another fibrosis model induced by ischemia-reperfusion injury. Adiponectin KO mice accumulated significantly fewer CD45^{+} myeloid fibroblasts in the kidney and developed much less interstitial collagen deposition after ischemia-reperfusion injury (Figure 7).

Adiponectin Promotes Monocyte-to-Fibroblast Transition *via* Activation of AMPK

We further investigated the signaling mechanisms by which adiponectin promotes myeloid fibroblast activation using an *in vitro* model system. To this end, mouse bone marrow–derived monocytes were incubated with recombinant adiponectin protein. Our results showed that adiponectin dose- and time-dependently induced α-SMA, fibronectin, and collagen I protein expression (Figure 8). These results indicate that these cells are capable of responding to adiponectin stimulation. We next examined whether adiponectin can activate AMP-activated protein kinase (AMPK), a downstream signaling molecule of adiponectin.[31] Our results demonstrated that adiponectin treatment led to phosphorylation of AMPKα in a time- and dose-dependent manner (Figure 9).

We next sought to explore whether inhibition of AMPK modulates adiponectin-induced monocyte-to-fibroblast transition and ECM protein production. To this end, bone marrow–derived monocytes were treated with compound C, a selective AMPK inhibitor. Incubation of bone marrow–derived monocytes with compound C at 10 μM abolished adiponectin-induced phosphorylation of AMPKα. Furthermore, compound C effectively blocked adiponectin-induced fibronectin, collagen I, and α-SMA expression in bone marrow–derived monocytes, as demonstrated by quantitative, real-time RT-PCR and Western blot analysis (Figure 10). Interestingly, compound C also significantly inhibited CD206 gene expression (Figure 10D). To verify that AMPK mediates the effect of adiponectin on monocyte-to-fibroblast transition, bone marrow–derived monocytes were transduced with a recombinant adenovirus expressing a dominant negative form of AMPKα (Ad-DN-AMPK). Cells transduced with a recombinant adenovirus expressing enhanced green fluorescent protein (GFP) were used as control. Forty-eight hours after transduction, cells were incubated with adiponectin at 10 μg/ml for 24 hours. Western blot analysis revealed that ectopic expression of hemagglutinin (HA)-tagged DN-AMPKα1 blocked adiponectin-induced phosphorylation of AMPKα (Figure 11, A and B). Consistently, expression of DN-AMPKα1 abolished adiponectin-induced fibronectin, collagen I, and α-SMA protein expression in bone marrow–derived monocytes (

Figure 11, C and D). Therefore, our results indicate that adiponectin induces monocyte-to-fibroblast transition and ECM protein production through AMPK activation.

To assess further the role of AMPK signaling in adiponectin-induced monocyte-to-fibroblast transition and ECM protein production, bone marrow–derived monocytes were incubated with 5-aminoimidazole-4-carboxamide-riboside (AICAR), a selective AMPK activator. Western blot analysis showed that AICAR induced phosphorylation of AMPKα and increased expression of fibronectin, collagen I, and α-SMA protein expression in bone marrow–derived monocytes in a time- and dose-dependent manner (Figures 12 and 13). These results indicate that activation of AMPK directly promotes monocyte-to-fibroblast transition and ECM protein production.

Discussion

Adiponectin is a multifunctional cytokine that modulates inflammation and metabolism. However, its role in renal fibrosis is unknown. In this study, we have demonstrated that adiponectin is induced in the kidney during the pathogenesis of renal fibrosis and that genetic deletion of adiponectin inhibits the accumulation of bone marrow–derived fibroblasts in the kidney after injury and suppresses chemokine and Th2 cytokine production, which is associated with a reduction of renal fibrosis. In cultured bone marrow–derived monocytes, adiponectin activates AMPK and induced α-SMA and extracellular matrix protein expression in a time- and dose-dependent manner. AMPK inhibition with a pharmacologic inhibitor or dominant negative AMPKα1 attenuated adiponectin-induced expression of α-SMA and extracellular matrix proteins. AMPK activation with AICAR increased expression of α-SMA and extracellular matrix proteins. These results indicate that adiponectin signaling plays a pivotal role in the pathogenesis of renal fibrosis by regulating monocyte-to-fibroblast transition.

Activated fibroblasts are effector cells that initiate and perpetuate fibrosis. Recent studies have shown that bone marrow–derived fibroblasts play a critical role in the pathogenesis of renal fibrosis.[7,10,12] The signaling mechanisms underlying the accumulation and activation of bone marrow–derived fibroblasts in the kidney are incompletely understood. We have previously shown that CXCL16 plays an obligatory role in the accumulation of myeloid fibroblasts in the kidney and the development of renal fibrosis in response to obstructive injury. The present study shows for the first time that adiponectin is pathologically important in the pathogenesis of renal fibrosis because targeted disruption of adiponectin inhibits macrophage polarization and causes a significant reduction of bone marrow–derived fibroblasts in the kidney in response to obstructive injury. These data indicate that adiponectin plays a critical role in M2 macrophage polarization and development of bone marrow–derived fibroblasts in the kidney.

Myofibroblasts are generally considered to be the main source of increased ECM deposition in renal fibrosis.[3–5] Experimental and clinical studies have shown that the number of interstitial myofibroblasts correlates closely with the severity of tubulointerstitial fibrosis and the progression of kidney disease.[32–34] In the present study, we demonstrate that myofibroblasts identified as α-SMA–positive cells accumulate in the kidney of WT mice after obstructive injury, and their accumulation is significantly reduced in the obstructed kidney of adiponectin KO mice. These results strongly indicate that adiponectin signaling plays an important role in the activation and maturation of bone marrow–derived fibroblasts in the kidney, which contribute to the population of renal myofibroblasts.

In response to injury, many cell types in the circulation are recruited to engage in a wound-healing response. A dysregulated wound healing process causes fibrosis, where ECM and fibroblasts replace normal parenchyma and lead to organ dysfunction. Fibrosis is a complex and progressive pathologic process involving infiltration of mononuclear cells, including fibrocytes, macrophages, and immune cells, suggesting that interaction and communication among these cell types regulates the pathogenesis of fibrotic disorders.[35,36] Therefore, understanding the interactions among these cells may identify novel therapeutic targets for the treatment of these devastating fibrotic disorders. The maturation of fibrocytes is

regulated by inflammatory cells such as T cells *via* secretion of cytokines.[12] Profibrotic cytokines IL-4 and IL-13 promote fibrocyte differentiation, whereas antifibrotic cytokines IFN-γ and IL-12 inhibit its differentiation, suggesting that a complex interplay in the inflamed milieu determines the fate of bone marrow–derived fibroblasts.[13,18] In this study, we show that adiponectin regulates macrophage polarization and myeloid fibroblast formation in the kidney in response to obstructive injury. To explore the mechanisms by which adiponectin promotes the activation of bone marrow–derived fibroblasts in the kidney in response to obstructive injury, we demonstrate that adiponectin deficiency significantly reduces the gene expression of profibrotic chemokines and cytokines in obstructed kidneys compared with WT mice. Th2 cytokines are profibrotic *in vivo* in other organs.[37,38] Furthermore, we and others have reported that Th2 cytokines promote monocyte-to-fibroblast transition.[12,13,18] Therefore, our results indicate that adiponectin induces profibrotic chemokine and Th2 cytokine production to promote monocyte-to-fibroblast transition.

It is generally thought that macrophages normally do not produce collagen. Macrophages promote fibrosis by producing an array of factors that activate fibroblasts.[39] Recently, a model of two major macrophage classes has developed. Classically activated macrophages exhibit a Th1-like phenotype, promoting inflammation in response to Th1 cytokines; while alternatively activated macrophages or M2 macrophages display a Th2-like phenotype, promoting ECM construction in response to Th2 cytokines.[29] M2 macrophages are characterized by elevated MHC class II, mannose receptor (CD206), Ym1, Fizz1/Relm-α, and arginase activity. Alternatively activated macrophages have been implicated in the pathogenesis of fibrosis in other organs[29] and repair after renal ischemia-reperfusion injury.[40] In our study, we demonstrate for the first time that alternatively activated macrophages produce procollagen I, suggesting a link between M2 macrophage polarization and monocyte-to-fibroblast transition. Consistent with this novel concept, adiponectin has been shown to promote M2 macrophage polarization *via* induction of Th2 cytokines.[41,42]

A key marker of renal fibrosis is the dramatic increase and deposition of extracellular matrix proteins, including collagen and fibronectin. Morphometric analysis of picrosirius red staining of kidney sections at day 14 after obstructive injury demonstrates the presence of interstitial collagen deposition. This collagen deposition is significantly attenuated in the obstructed kidney of adiponectin KO mice. Consistent with these findings, we further show that the expression of collagen I and fibronectin are markedly increased in the injured kidney of WT mice, whereas these fibrotic responses are significantly attenuated in the injured kidney of adiponectin KO mice.

Adiponectin exerts its action through interaction with two receptors, AdipoR1 and AdipoR2.[43] Both AdipoR1 and AdipoR2 are seven-transmembrane receptors that are structurally and functionally distinct from G protein–coupled receptors.[44] Adiponectin receptors are biologically active and bind to an adaptor protein containing a pleckstrin-homology domain, a phosphotyrosine-binding domain, and a leucine zipper motif (APPL1)[45] Through the stimulation of AdipoR1 and AdipoR2, adiponectin has been reported to activate AMPK.[31] AMPK is a heterotrimeric protein composed of α, β, and γ subunits. Adiponectin has been recognized as a critical regulator of energy metabolism and inflammation.[46] In our study, we demonstrate that AMPK is a primary mediator of adiponectin-induced monocyte-to-fibroblast transition and matrix protein expression in bone marrow–derived monocytes. Inhibition of AMPK with a pharmacologic inhibitor or ectopic expression of dominant negative AMPKα abolished the ability of adiponectin to induce monocyte-to-fibroblast transition and matrix protein expression. Furthermore, activation of AMPK with AICAR promotes monocyte-to-fibroblast transition and matrix protein expression. These results indicate that AMPK signaling mediates adiponectin-induced monocyte-to-fibroblast transition and matrix protein expression.

In summary, our study defines a novel mechanism by which adiponectin regulates the pathogenesis of renal fibrosis. In response to injury, adiponectin leads to Th2 cytokine production and monocyte-to-fibroblast transition, which contribute significantly to the pathogenesis of renal interstitial fibrosis. These

data suggest that inhibition of adiponectin/AMPK signaling may represent a novel therapeutic approach for chronic fibrotic kidney disease.

Concise Methods

Animals

Animal experiments were approved by the Institutional Animal Care and Use Committee of Baylor College of Medicine. WT C57BL/6 mice were purchased from the Jackson Laboratory (Bar Harbor, ME). The adiponectin KO mouse on a background of C57BL/6J was generated as previously described.[47] Male WT or adiponectin KO mice (8–12 weeks old, weighing 20–30 g) were anesthetized by intraperitoneal injection of ketamine (80 mg/kg) and xylazine (10 mg/kg). Through a flank incision, the left ureter was exposed and completely ligated using fine suture material (4-0 silk) at two points as described.[10] To induce unilateral ischemia-reperfusion injury, left kidneys were exposed through flank incision and were subjected to ischemia by clamping renal pedicles with nontraumatic micro aneurysm clamps. After 45 minutes, the clamps were removed and blood reflow was confirmed. Body temperature was maintained at 36.5–37.5°C throughout the procedure. Mice were allowed to recover from anesthesia and were housed in standard rodent cages with *ad libitum* access to water and food until euthanized.

Renal Morphology

Mice were euthanized and perfused by injections of PBS into the left ventricle of the heart to remove blood. One portion of the renal tissue was fixed in 10% buffered formalin and embedded in paraffin, cut at 4-μm thickness, and stained with hematoxylin and eosin for initial evaluation or picrosirius red staining to identify collagen fibers. The picrosirius red-stained sections were scanned using a microscope equipped with a digital camera (Nikon, Melville, NY), and quantitative evaluation was performed using NIS-Elements Br 3.0 software. The collagen-stained area was calculated as a percentage of the total area.

Quantitative Real-Time RT-PCR

Quantitative analysis of the target mRNA expression was performed with real-time RT-PCR by the relative standard curve method.[10] Total RNA was extracted from snap-frozen kidney tissues with TRIzol Reagent (Invitrogen). Total RNA were reverse-transcribed and amplified in triplicate using IQ SYBR green supermix reagent (Bio-Rad, Hercules, CA) with a real-time PCR machine (Bio-Rad, Hercules, CA), according to the manufacturer's instructions. The specificity of real-time PCR was confirmed using melting-curve analysis. The expression levels of the target genes were normalized by the glyceraldehyde 3-phosphate dehydrogenase (GAPDH) level in each sample. The following are the primer sequences. Adiponectin: forward 5′-CACACCAGGCCGTGATGGCAGA-3′ and reverse 5′-TCCTTTCCTGCCAGGGGTTCCG-3′; MCP-1: forward 5′-TCACCTGCTGCTACTCATTCACCA-3′ and reverse 5′- TACAGCTTCTTTGGGACACCTGCT-3′; CXCL16: forward 5′-ACCCTTGTCTCTTGCGTTCTTCCT-3′ and reverse 5′- ATGTGATCCAAAGTACCCTGCGGT-3′; IL-13: forward 5′- CAGCCTCCCCGATACCAAAAT-3′ and reverse 5′-GCGAAACAGTTGCTTTGTGTAG-3′; IL-4: forward 5′-ATCGGCATTTTGAACGAGGTC-3′ and reverse 5′-GAGGACGTTTGGCACATCCA-3′; CD206: forward 5′- GCTTCTGCCCCATCAAGAGTA-3′ and reverse 5′- AGGACAGTGTGGATTGGAAGT-3′; collagen I: forward 5′-TGCCGCGACCTCAAGATGTG-3′ and reverse 5′-CACAAGGGTGCTGTAGGTGA-3′; fibronectin: forward 5′-CTTCTCCGTGGAGTTTTACCG-3′ and reverse 5′- GCTGTCAAATTGAATGGTGGTG-3′; α-SMA: forward 5′-ACTGGGACGACATGGAAAAG-3′ and reverse 5′-CATCTCCAGAGTCCAGCACA-3′; GAPDH: forward 5′-TGCTGAGTATGTCGTGGAGTCTA-3′ and reverse 5′-AGTGGGAGTTGCTGTTGAAATC-3′.

Immunohistochemistry

Immunohistochemical staining for adiponectin was performed on paraffin sections using a goat antiadiponectin antibody (R & D System). Antigen retrieval was performed with antigen unmasking solution (Vector Laboratories, Burlingame, CA). Endogenous peroxidase activity was quenched with 3% H_2O_2. After blocked with 5% normal serum, sections were incubated with primary antibodies in a humidified chamber overnight. After washing, sections were incubated with an antigoat antibody and ABC solution sequentially according to the ABC kit (Vector Laboratories). Immunoreactivity was then visualized by incubating sections in 3,3′-diaminobenzidine solution for an appropriate period of time. Nuclear staining was performed with hematoxylin. The slides were dehydrated, cleared, and mounted. The images from these slides were acquired and analyzed by NIS Element software with a Nikon microscope image system.

Immunofluorescence

Frozen kidney sections were fixed and nonspecific binding was blocked with protein block (DAKO). Sections were then incubated with rabbit anticollagen I antibody (Rockland) followed by Alexa-488 conjugated donkey antirabbit antibody (Invitrogen), and rabbit antifibronectin antibody (Sigma), followed by Alexa-488 conjugated donkey antirabbit antibody (Invitrogen), or rabbit anti–α-SMA antibody (Abcam) followed by Alexa-488 conjugated donkey antirabbit antibody (Invitrogen). For double immunofluorescence, kidney section were fixed and stained with primary antibodies followed by appropriate secondary antibodies sequentially. Slides were mounted with mounting medium containing DAPI. Fluorescence intensity was visualized using a microscope equipped with a digital camera (Nikon). Sections stained with antibodies to fibronectin, collagen I, and α-SMA were quantitatively evaluated using NIS-Elements Br 3.0 software. The fluorescence positive area was calculated as a percentage of the total area.[10]

Renal Cell Isolation and Flow Cytometry

Renal cell isolation and flow cytometry were performed as described.[10] Briefly, kidney was minced and incubated at 37°C for 30 minutes in PBS containing Liberase TM (Roche) and DNase (Roche). Cells were filtered through a 40-μm strainer, washed, centrifuged, and resuspended in FACS buffer. Cells (5×10^5) were fixed and permeabilized using the Cytofix/Cytoperm kit (BD Biosciences, San Jose, CA) in accordance with the manufacturer's protocol, then incubated with FITC–anti-CD45 (BD Biosciences) and biotin–anti-collagen I (Rockland, Gilbertsville, PA)/streptavidin-APC (BD Biosciences). Cells incubated with irrelevant isotype-matched antibodies (BD Biosciences) and unstained cells were used as controls. The cutoffs were set according to results of controls. The fluorescence intensities were measured using a BD LSR II flow cytometer (BD Biosciences). Data were analyzed using BD FACSDiva software.

Bone Marrow–Derived Monocyte Culture and Treatment

Mouse bone marrow–derived monocytes were isolated and cultured according to a published protocol.[48] Briefly, bone marrow–derived monocytes were isolated from the femur and tibia of 8- to 12-week-old mice, passed through a 40-μm cell strainer (BD Falcon), and cultured in RPMI medium containing 10% FBS, 10% L929 conditioned medium, 1% glutamine, 1% MEM vitamins, and 1% penicillin/streptomycin in a humid incubator at 37°C and 5% CO_2. Fresh medium was replaced every 2–3 days. More than 98% of the cells were stained positive for CD11b and F4/80. These cells were then treated with recombinant mouse full-length adiponectin expressed in HEK293 cells (BioVendor) or vehicle in the presence or absence of compound C or AICAR. Recombinant adenovirus encoding HA-tagged dominant negative AMPKα1 (Ad-DN-AMPKα) was purchased from Eton Bioscience. Cells were transduced with Ad-DN AMPKα or adenovirus expressing GFP (Ad-GFP) at a multiplicity of infection of 100. Forty-eight hours after transduction, cells were treated with recombinant mouse full-length adiponectin or vehicle for 24

hours. Expression of HA-tagged DN-AMPKα was confirmed by Western blot with antibody against HA (Rockland).

Western Blot Analysis

Protein was extracted using the radioimmunoprecipitation assay buffer containing a cocktail of proteinase inhibitors (Thermo Fisher Scientific Inc., Rockford, IL) and quantified with a Bio-Rad protein assay. Equal amounts of protein were separated on SDS-polyacrylamide gels in a Tris/HCl buffer system, transferred onto nitrocellulose membranes, and blotted according to standard procedures with primary antibodies against adiponectin, collagen I, fibronectin, α-SMA, HA, p-AMPKα (phosphorylated-AMPKα), AMPKα, or GAPDH. The specific bands of target proteins were analyzed using an Odyssey IR scanner (LI-COR Bioscience, Lincoln, NE) and band intensities were quantified using NIH Image/J.

Statistical Analysis

All data were expressed as mean ± SEM. Multiple group comparisons were performed by one-way ANOVA followed by the Bonferroni procedure for comparison of means. Comparisons between two groups were analyzed by the two-tailed t test. $P<0.05$ was considered to represent a statistically significant finding.

Disclosures

None.

Footnotes

Published online ahead of print. Publication date available at www.jasn.org.

References

1. Schainuck LI, Striker GE, Cutler RE, Benditt EP: Structural-functional correlations in renal disease. II. The correlations. Hum Pathol 1: 631–641, 1970 [PubMed: 5521736]

2. Nath KA: The tubulointerstitium in progressive renal disease. Kidney Int 54: 992–994, 1998 [PubMed: 9734628]

3. Neilson EG: Mechanisms of disease: Fibroblasts—a new look at an old problem. Nat Clin Pract Nephrol 2: 101–108, 2006 [PubMed: 16932401]

4. Strutz F, Müller GA: Renal fibrosis and the origin of the renal fibroblast. Nephrol Dial Transplant 21: 3368–3370, 2006 [PubMed: 16887850]

5. Liu Y: Renal fibrosis: New insights into the pathogenesis and therapeutics. Kidney Int 69: 213–217, 2006 [PubMed: 16408108]

6. Iwano M, Plieth D, Danoff TM, Xue C, Okada H, Neilson EG: Evidence that fibroblasts derive from epithelium during tissue fibrosis. J Clin Invest 110: 341–350, 2002 [PMCID: PMC151091] [PubMed: 12163453]

7. Sakai N, Wada T, Yokoyama H, Lipp M, Ueha S, Matsushima K, Kaneko S: Secondary lymphoid tissue chemokine (SLC/CCL21)/CCR7 signaling regulates fibrocytes in renal fibrosis. Proc Natl Acad Sci U S A 103: 14098–14103, 2006 [PMCID: PMC1599918] [PubMed: 16966615]

8. Grimm PC, Nickerson P, Jeffery J, Savani RC, Gough J, McKenna RM, Stern E, Rush DN: Neointimal and tubulointerstitial infiltration by recipient mesenchymal cells in chronic renal-allograft rejection. N Engl J Med 345: 93–97, 2001 [PubMed: 11450677]

9. Broekema M, Harmsen MC, van Luyn MJ, Koerts JA, Petersen AH, van Kooten TG, van Goor H, Navis G, Popa ER: Bone marrow-derived myofibroblasts contribute to the renal interstitial myofibroblast population and produce procollagen I after ischemia/reperfusion in rats. J Am Soc Nephrol 18: 165–175, 2007 [PubMed: 17135399]

10. Chen G, Lin SC, Chen J, He L, Dong F, Xu J, Han S, Du J, Entman ML, Wang Y: CXCL16 recruits bone marrow-derived fibroblast precursors in renal fibrosis. J Am Soc Nephrol 22: 1876–1886, 2011 [PMCID: PMC3187185] [PubMed: 21816936]

11. Bucala R, Spiegel LA, Chesney J, Hogan M, Cerami A: Circulating fibrocytes define a new leukocyte subpopulation that mediates tissue repair. Mol Med 1: 71–81, 1994 [PMCID: PMC2229929] [PubMed: 8790603]

12. Niedermeier M, Reich B, Rodriguez Gomez M, Denzel A, Schmidbauer K, Göbel N, Talke Y, Schweda F, Mack M: CD4+ T cells control the differentiation of Gr1+ monocytes into fibrocytes. Proc Natl Acad Sci U S A 106: 17892–17897, 2009 [PMCID: PMC2764893] [PubMed: 19815530]

13. Shao DD, Suresh R, Vakil V, Gomer RH, Pilling D: Pivotal Advance: Th-1 cytokines inhibit, and Th-2 cytokines promote fibrocyte differentiation. J Leukoc Biol 83: 1323–1333, 2008 [PMCID: PMC2659591] [PubMed: 18332234]

14. Haudek SB, Trial J, Xia Y, Gupta D, Pilling D, Entman ML: Fc receptor engagement mediates differentiation of cardiac fibroblast precursor cells. Proc Natl Acad Sci U S A 105: 10179–10184, 2008 [PMCID: PMC2465805] [PubMed: 18632582]

15. Metz CN: Fibrocytes: A unique cell population implicated in wound healing. Cell Mol Life Sci 60: 1342–1350, 2003 [PubMed: 12943223]

16. Quan TE, Cowper S, Wu SP, Bockenstedt LK, Bucala R: Circulating fibrocytes: Collagen-secreting cells of the peripheral blood. Int J Biochem Cell Biol 36: 598–606, 2004 [PubMed: 15010326]

17. Abe R, Donnelly SC, Peng T, Bucala R, Metz CN: Peripheral blood fibrocytes: Differentiation pathway and migration to wound sites. J Immunol 166: 7556–7562, 2001 [PubMed: 11390511]

18. Cieslik KA, Taffet GE, Carlson S, Hermosillo J, Trial J, Entman ML: Immune-inflammatory dysregulation modulates the incidence of progressive fibrosis and diastolic stiffness in the aging heart. J Mol Cell Cardiol 50: 248–256, 2011 [PMCID: PMC3019252] [PubMed: 20974150]

19. Tilg H, Moschen AR: Adipocytokines: Mediators linking adipose tissue, inflammation and immunity. Nat Rev Immunol 6: 772–783, 2006 [PubMed: 16998510]

20. Karbowska J, Kochan Z: Role of adiponectin in the regulation of carbohydrate and lipid metabolism. J Physiol Pharmacol 57[Suppl 6]: 103–113, 2006 [PubMed: 17228091]

21. Scherer PE, Williams S, Fogliano M, Baldini G, Lodish HF: A novel serum protein similar to C1q, produced exclusively in adipocytes. J Biol Chem 270: 26746–26749, 1995 [PubMed: 7592907]

22. Wolf AM, Wolf D, Avila MA, Moschen AR, Berasain C, Enrich B, Rumpold H, Tilg H: Up-regulation of the anti-inflammatory adipokine adiponectin in acute liver failure in mice. J Hepatol 44: 537–543, 2006 [PubMed: 16310276]

23. Crawford LJ, Peake R, Price S, Morris TC, Irvine AE: Adiponectin is produced by lymphocytes and is a negative regulator of granulopoiesis. J Leukoc Biol 88: 807–811, 2010 [PubMed: 20643815]

24. Katsiougiannis S, Kapsogeorgou EK, Manoussakis MN, Skopouli FN: Salivary gland epithelial cells: A new source of the immunoregulatory hormone adiponectin. Arthritis Rheum 54: 2295–2299, 2006 [PubMed: 16802369]

25. Miller M, Cho JY, Pham A, Ramsdell J, Broide DH: Adiponectin and functional adiponectin receptor 1 are expressed by airway epithelial cells in chronic obstructive pulmonary disease. J Immunol 182: 684–691, 2009 [PubMed: 19109202]

26. Becker B, Kronenberg F, Kielstein JT, Haller H, Morath C, Ritz E, Fliser D, MMKD Study Group : Renal insulin resistance syndrome, adiponectin and cardiovascular events in patients with kidney disease: The mild and moderate kidney disease study. J Am Soc Nephrol 16: 1091–1098, 2005 [PubMed: 15743998]

27. Stenvinkel P: Adiponectin in chronic kidney disease: A complex and context sensitive clinical situation. J Ren Nutr 21: 82–86, 2011 [PubMed: 21195926]

28. Haudek SB, Cheng J, Du J, Wang Y, Hermosillo-Rodriguez J, Trial J, Taffet GE, Entman ML: Monocytic fibroblast precursors mediate fibrosis in angiotensin-II-induced cardiac hypertrophy. J Mol Cell Cardiol 49: 499–507, 2010 [PMCID: PMC2917526] [PubMed: 20488188]

29. Gordon S, Martinez FO: Alternative activation of macrophages: Mechanism and functions. Immunity 32: 593–604, 2010 [PubMed: 20510870]

30. Ricardo SD, van Goor H, Eddy AA: Macrophage diversity in renal injury and repair. J Clin Invest 118: 3522–3530, 2008 [PMCID: PMC2575702] [PubMed: 18982158]

31. Heiker JT, Kosel D, Beck-Sickinger AG: Molecular mechanisms of signal transduction via adiponectin and adiponectin receptors. Biol Chem 391: 1005–1018, 2010 [PubMed: 20536390]

32. Zhang G, Moorhead PJ, el Nahas AM: Myofibroblasts and the progression of experimental glomerulonephritis. Exp Nephrol 3: 308–318, 1995 [PubMed: 7583053]

33. Roberts IS, Burrows C, Shanks JH, Venning M, McWilliam LJ: Interstitial myofibroblasts: Predictors of progression in membranous nephropathy. J Clin Pathol 50: 123–127, 1997 [PMCID: PMC499736] [PubMed: 9155692]

34. Essawy M, Soylemezoglu O, Muchaneta-Kubara EC, Shortland J, Brown CB, el Nahas AM: Myofibroblasts and the progression of diabetic nephropathy. *Nephrol Dial Transplant* 12: 43–50, 1997

35. Wynn TA: Cellular and molecular mechanisms of fibrosis. J Pathol 214: 199–210, 2008 [PMCID: PMC2693329] [PubMed: 18161745]

36. Kisseleva T, Brenner DA: Mechanisms of fibrogenesis. Exp Biol Med (Maywood) 233: 109–122, 2008 [PubMed: 18222966]

37. Cheever AW, Williams ME, Wynn TA, Finkelman FD, Seder RA, Cox TM, Hieny S, Caspar P, Sher A: Anti-IL-4 treatment of Schistosoma mansoni-infected mice inhibits development of T cells and non-B,

non-T cells expressing Th2 cytokines while decreasing egg-induced hepatic fibrosis. J Immunol 153: 753–759, 1994 [PubMed: 8021510]

38. Finkelman FD, Wynn TA, Donaldson DD, Urban JF: The role of IL-13 in helminth-induced inflammation and protective immunity against nematode infections. Curr Opin Immunol 11: 420–426, 1999 [PubMed: 10448138]

39. Wynn TA, Barron L: Macrophages: Master regulators of inflammation and fibrosis. Semin Liver Dis 30: 245–257, 2010 [PMCID: PMC2924662] [PubMed: 20665377]

40. Lee S, Huen S, Nishio H, Nishio S, Lee HK, Choi BS, Ruhrberg C, Cantley LG: Distinct macrophage phenotypes contribute to kidney injury and repair. J Am Soc Nephrol 22: 317–326, 2011 [PMCID: PMC3029904] [PubMed: 21289217]

41. Mandal P, Pratt BT, Barnes M, McMullen MR, Nagy LE: Molecular mechanism for adiponectin-dependent M2 macrophage polarization: Link between the metabolic and innate immune activity of full-length adiponectin. J Biol Chem 286: 13460–13469, 2011 [PMCID: PMC3075692] [PubMed: 21357416]

42. Ohashi K, Parker JL, Ouchi N, Higuchi A, Vita JA, Gokce N, Pedersen AA, Kalthoff C, Tullin S, Sams A, Summer R, Walsh K: Adiponectin promotes macrophage polarization toward an anti-inflammatory phenotype. J Biol Chem 285: 6153–6160, 2010 [PMCID: PMC2825410] [PubMed: 20028977]

43. Yamauchi T, Kamon J, Ito Y, Tsuchida A, Yokomizo T, Kita S, Sugiyama T, Miyagishi M, Hara K, Tsunoda M, Murakami K, Ohteki T, Uchida S, Takekawa S, Waki H, Tsuno NH, Shibata Y, Terauchi Y, Froguel P, Tobe K, Koyasu S, Taira K, Kitamura T, Shimizu T, Nagai R, Kadowaki T: Cloning of adiponectin receptors that mediate antidiabetic metabolic effects. Nature 423: 762–769, 2003 [PubMed: 12802337]

44. Kadowaki T, Yamauchi T: Adiponectin and adiponectin receptors. Endocr Rev 26: 439–451, 2005 [PubMed: 15897298]

45. Mao X, Kikani CK, Riojas RA, Langlais P, Wang L, Ramos FJ, Fang Q, Christ-Roberts CY, Hong JY, Kim RY, Liu F, Dong LQ: APPL1 binds to adiponectin receptors and mediates adiponectin signalling and function. Nat Cell Biol 8: 516–523, 2006 [PubMed: 16622416]

46. Steinberg GR, Kemp BE: AMPK in health and disease. Physiol Rev 89: 1025–1078, 2009 [PubMed: 19584320]

47. Ma K, Cabrero A, Saha PK, Kojima H, Li L, Chang BH, Paul A, Chan L: Increased beta -oxidation but no insulin resistance or glucose intolerance in mice lacking adiponectin. J Biol Chem 277: 34658–34661, 2002 [PubMed: 12151381]

48. Weischenfeldt J, Porse B: Bone marrow-derived macrophages (BMM): isolation and applications. *CSH Protoc,* 2008**:** pdb prot5080, 2008

Figures and Tables

Figure 1.
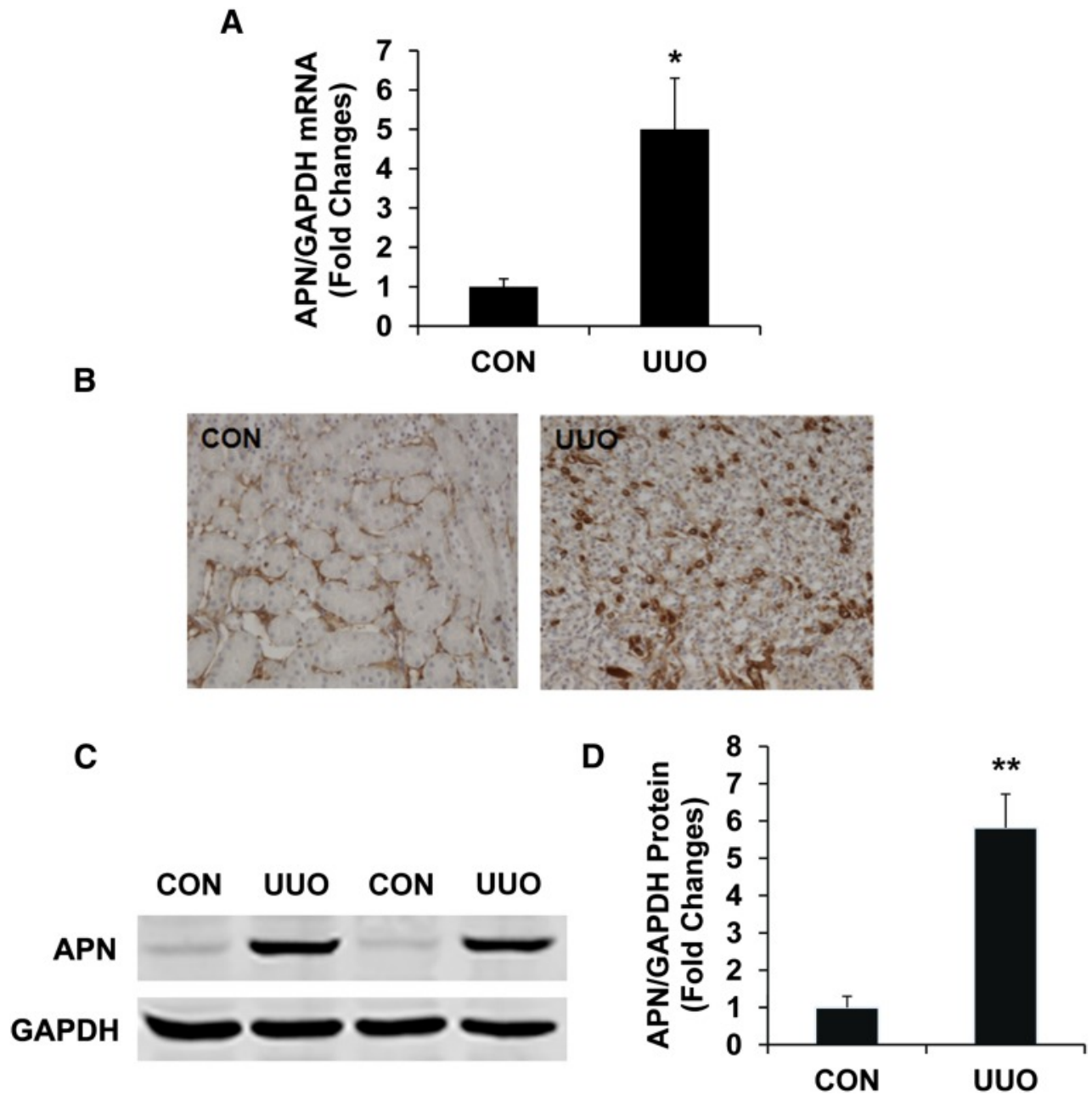
Adiponectin is induced in the kidney after obstructive injury. (A) Graphic presentation shows adiponectin mRNA induction. *$P<0.05$ versus normal control kidney. $n=4$ per group. (B) Representative photomicrographs of kidney sections stained for adiponectin (brown) and counterstained with hematoxylin (blue) (original magnification, ×400). (C) Representative Western blots show the protein levels of adiponectin in control (CON) and UUO kidneys of WT mice. (D) Quantitative analysis of adiponectin protein expression in the control and UUO kidneys of WT mice. **$P<0.01$ versus WT controls. $n=4$ per group. APN, adiponectin.

Figure 2.
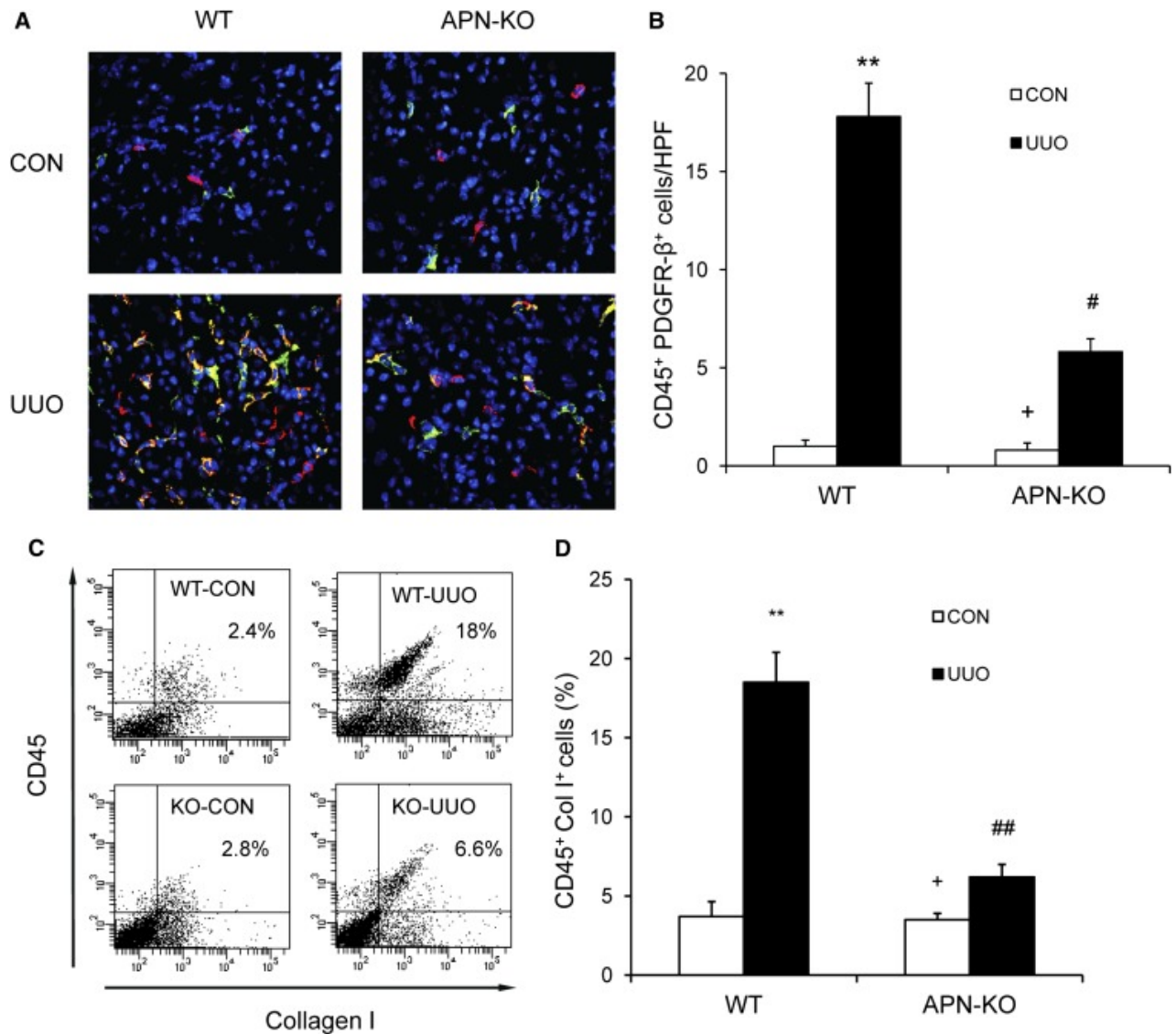
Adiponectin deficiency suppresses the accumulation of bone marrow–derived fibroblasts in the kidney after obstructive injury. (A) Representative photomicrographs of kidney sections from WT and adiponectin KO mice 7 days after UUO stained for CD45 (red), PDGFR-β (green), and DAPI (blue) (original magnification, ×400). (B) Quantitative analysis of CD45 and PDGFR-β dual-positive fibroblasts in the kidneys in response to UUO. **$P<0.01$ versus WT control, [+]$P<0.05$ versus KO UUO, and [#]$P<0.05$ versus WT UUO. n=5–6 per group. (C) Representative cytometric diagrams showing the effect of adiponectin deficiency on the accumulation of CD45 and collagen I dual-positive fibroblasts in the kidney in response to UUO. (D) Quantitative analysis of CD45 and collagen I dual-positive fibroblasts in the kidneys in response to UUO. **$P<0.01$ versus WT control (CON), [+]$P<0.05$ versus KO UUO, and [##]$P<0.01$ versus WT UUO. n=4 per group. APN, adiponectin.

Figure 3.
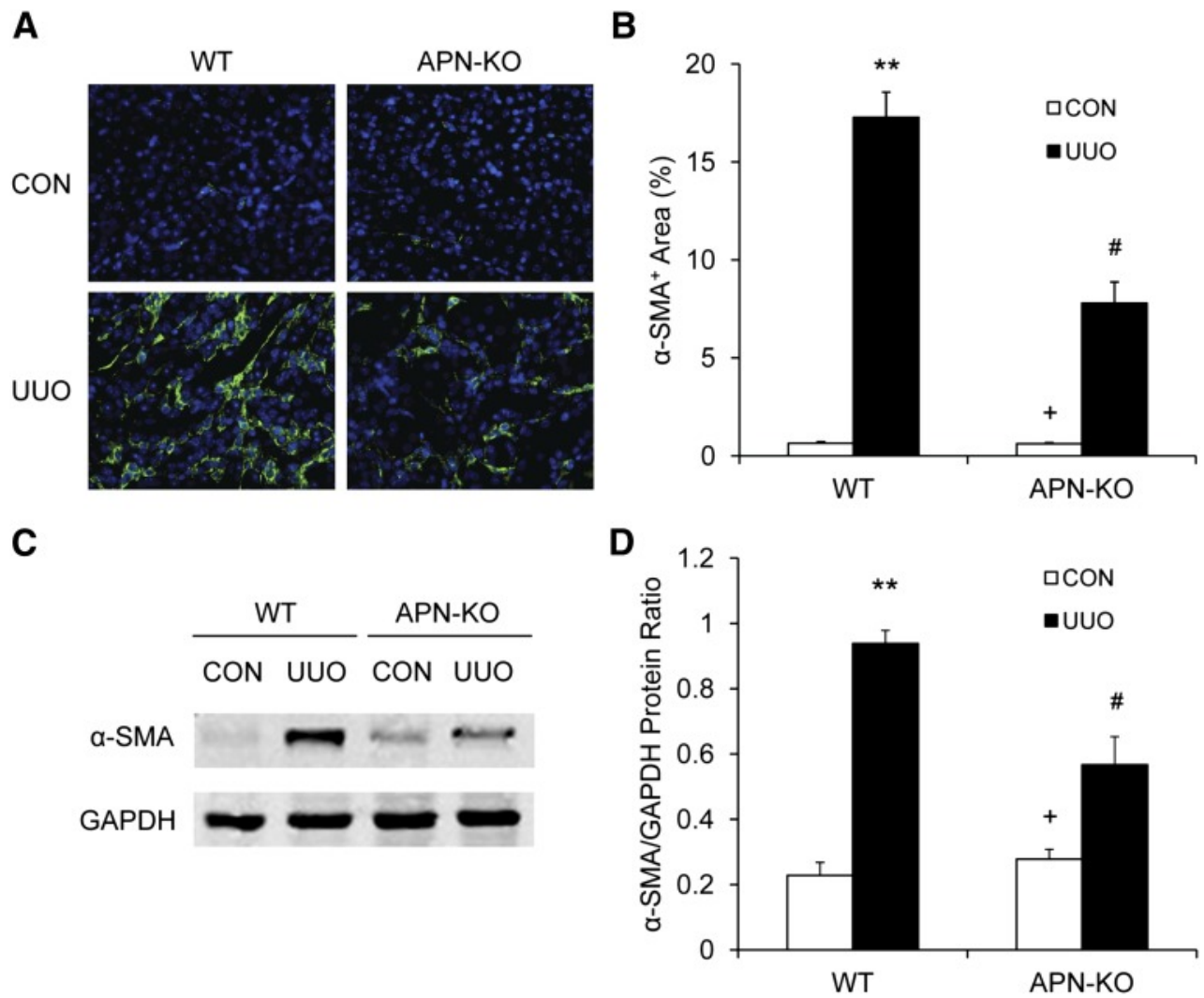
Adiponectin deficiency inhibits myofibroblast formation in the kidney. (A) Representative photomicrographs of α-SMA immunofluorescent staining in the kidneys of WT and adiponectin KO mice 1 week after UUO (original magnification, ×400). (B) Quantitative analysis of α-SMA protein expression in the kidneys of WT and adiponectin KO mice 1 week after UUO. **$P<0.01$ versus WT controls (CON), [+]$P<0.05$ versus KO UUO, and [#]$P<0.05$ versus WT UUO. $n=5$–6 per group. (C) Representative Western blots show the levels of α-SMA protein expression in the kidneys of WT and adiponectin KO mice. (D) Quantitative analysis of α-SMA protein expression in the kidneys of WT and adiponectin KO mice. **$P<0.01$ versus WT controls, [+]$P<0.05$ versus KO UUO, and [#]$P<0.05$ versus WT UUO. $n=4$ per group. APN, adiponectin.

Figure 4.
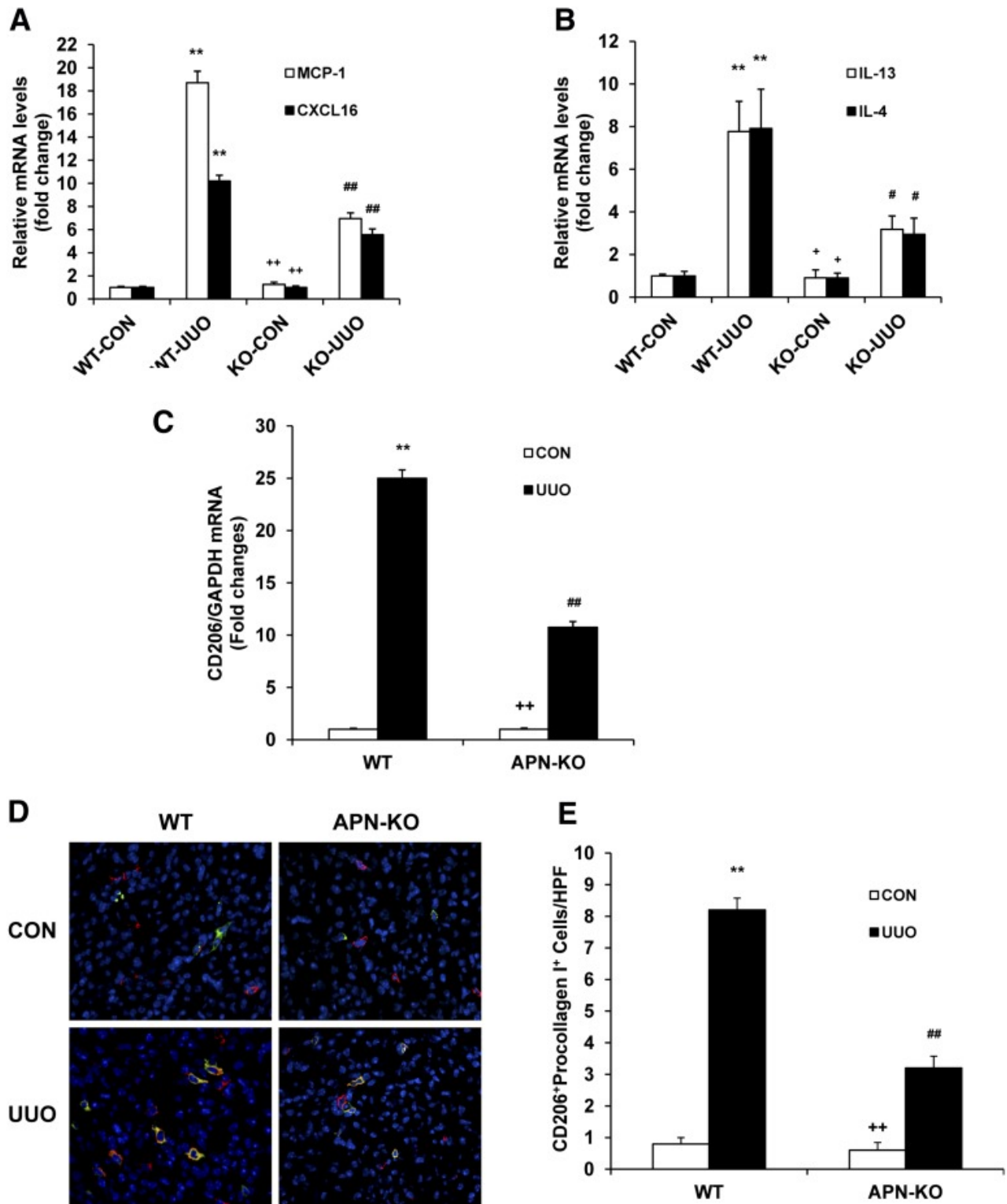
Adiponectin deficiency attenuates profibrotic chemokine and cytokine production and M2 macrophage polarization. (A) The mRNA levels of MCP-1 and CXCL16 in the kidneys of WT and adiponectin KO mice as determined by real-time RT-PCR. **$P<0.01$ versus WT control (CON), [++]$P<0.01$ versus KO UUO, and [##]$P<0.01$ versus WT UUO. $n=4$ per group. (B) The mRNA levels of IL-13 and IL-4 in the kidneys of WT and adiponectin KO mice as determined by real-time RT-PCR. **$P<0.01$ versus WT control, [+]$P<0.05$ versus KO UUO, and [#]$P<0.05$ versus WT UUO. $n=4$ per group. (C) The mRNA levels of CD206 in the kidney of WT and adiponectin KO mice as determined by real-time RT-PCR. **$P<0.01$ versus WT control, [++]$P<0.01$ versus KO UUO, and [##]$P<0.01$ versus WT UUO. $n=4$ per group. (D) Representative photomicrographs show kidney sections stained with CD206 (red) and procollagen I (green), counterstained with DAPI (blue), and examined with a fluorescence microscope. (E) Quantitative analysis of CD206 and procollagen I dual-positive

cells in the kidneys. **$P<0.01$ versus WT control, [++]$P<0.01$ versus KO UUO, and [##]$P<0.01$ versus WT UUO. $n=5–6$ per group. APN, adiponectin.

Figure 5.
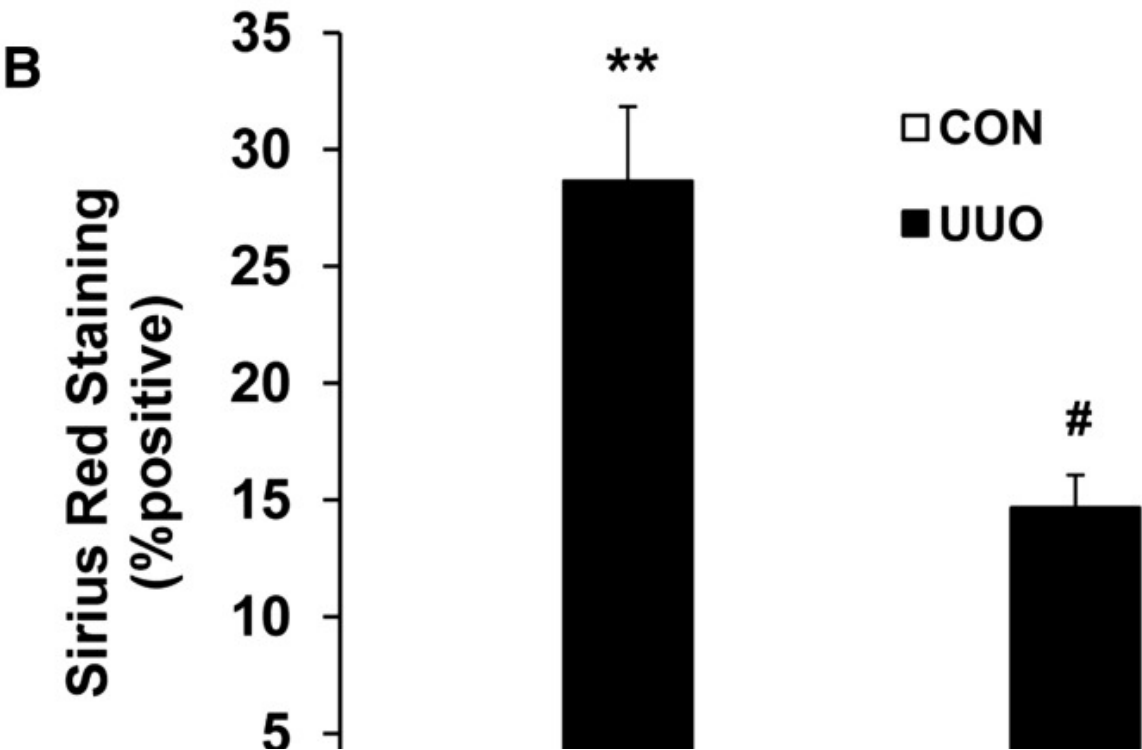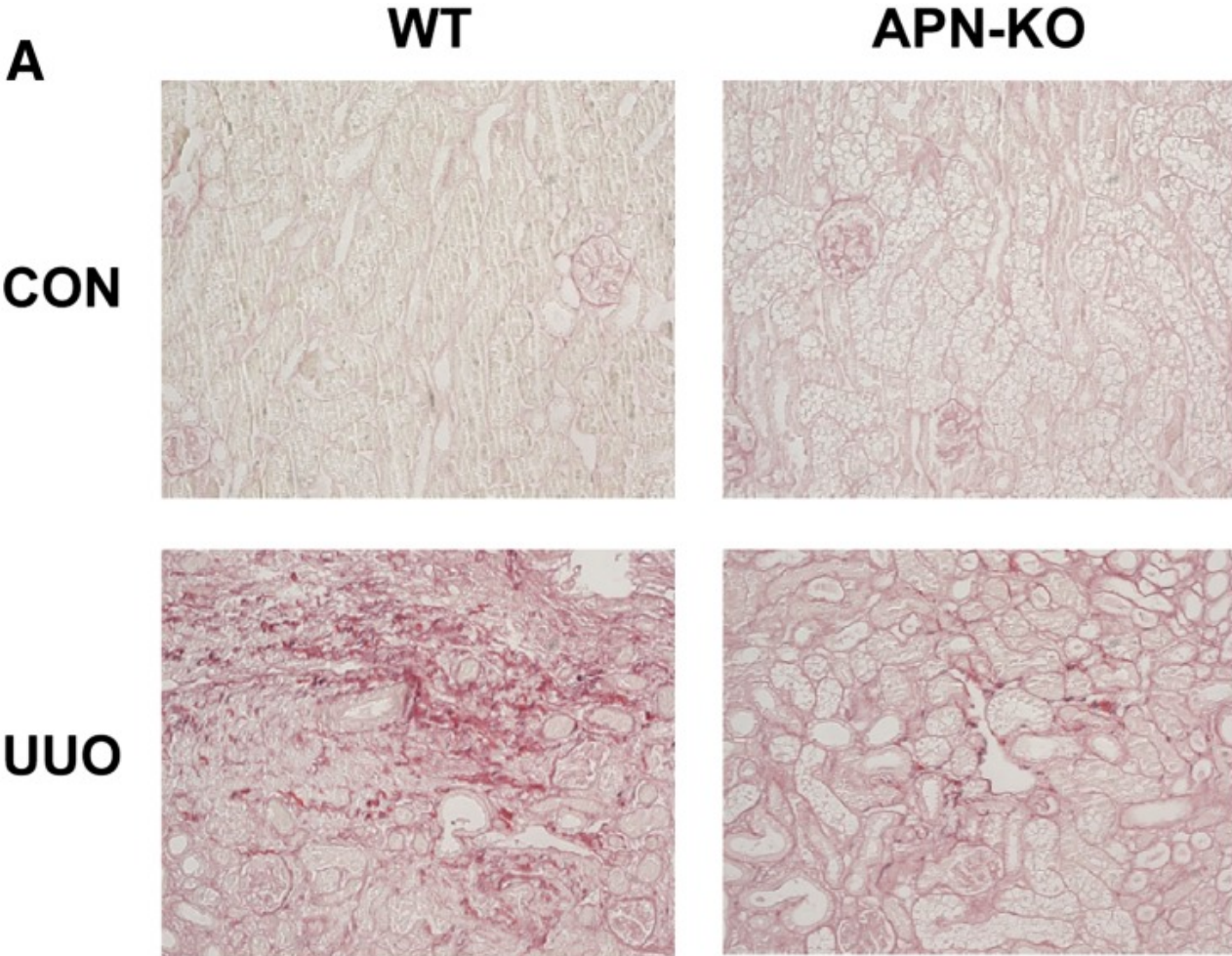
Adiponectin deficiency attenuates renal fibrosis and extracellular matrix deposition. (A) Representative photomicrographs show kidney sections stained with picrosirius red for assessment of total collagen deposition (original magnification, ×200). (B) Quantitative analysis of renal interstitial collagen content in different groups as indicated. **$P<0.01$ versus WT controls, [+]$P<0.05$ versus KO UUO, and [#]$P<0.05$ versus WT UUO. $n=5$–6 per group. APN, adiponectin, CON, control.

Figure 6.
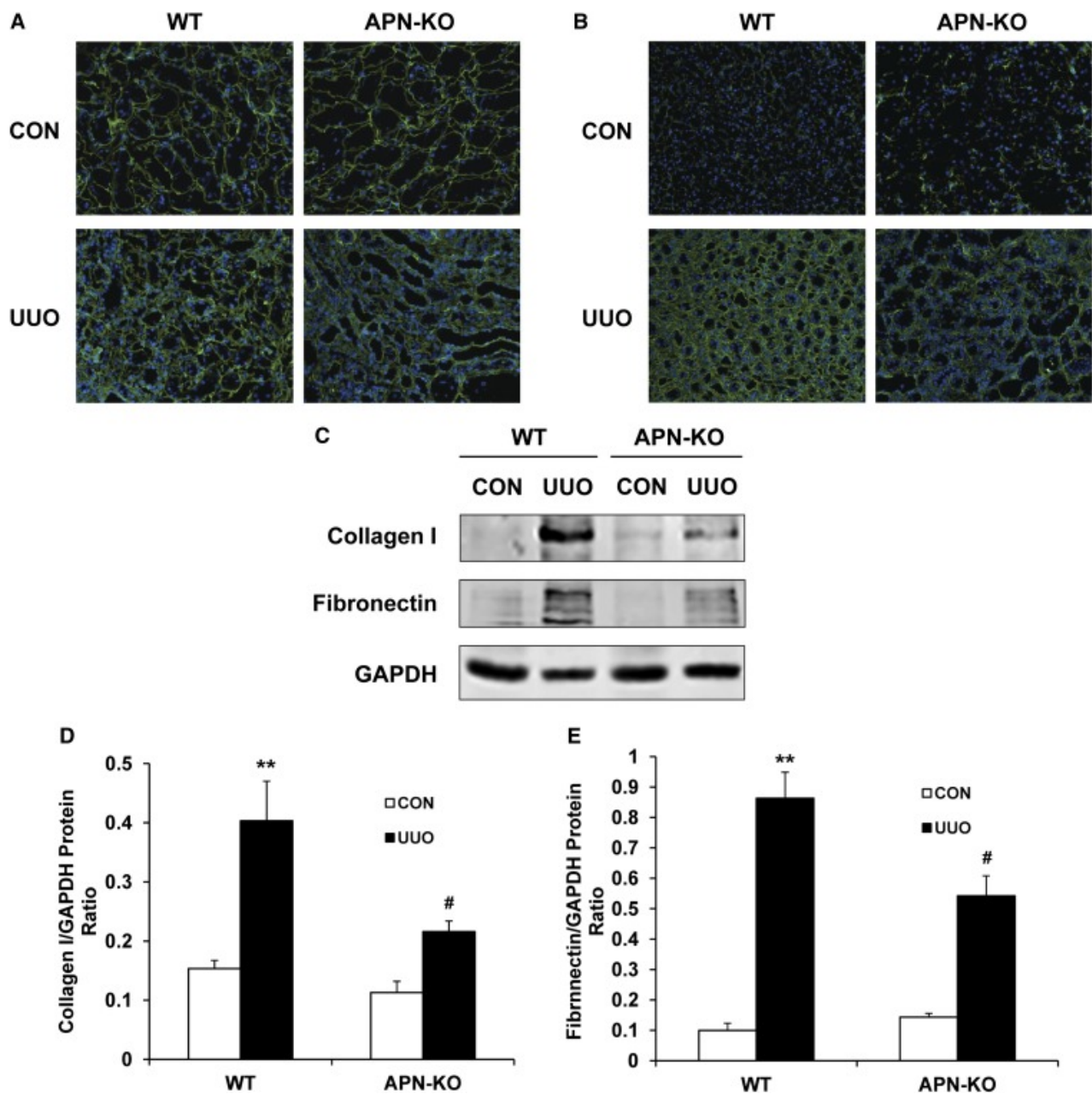
Adiponectin deficiency inhibits collagen I and fibronectin expression. (A) Representative photomicrographs of collagen I immunostaining in the kidneys of WT and adiponectin KO mice at day 14 after surgery (original magnification, ×200). (B) Representative photomicrographs of fibronectin immunostaining in the kidneys of WT and adiponectin KO mice at

day 14 after surgery (original magnification, ×200). (C) Representative Western blots show the protein levels of collagen I and fibronectin in the kidneys of WT and adiponectin KO mice. (D) Quantitative analysis of collagen I protein expression in the kidney of WT and adiponectin KO mice. **$P<0.01$ versus WT controls and #$P<0.05$ versus WT UUO. $n=4$ per group. (E) Quantitative analysis of fibronectin protein expression in the kidney of WT and adiponectin KO mice. **$P<0.01$ versus WT controls and #$P<0.05$ versus WT UUO. $n=4$ per group. APN, adiponectin, CON, control.

Figure 7.
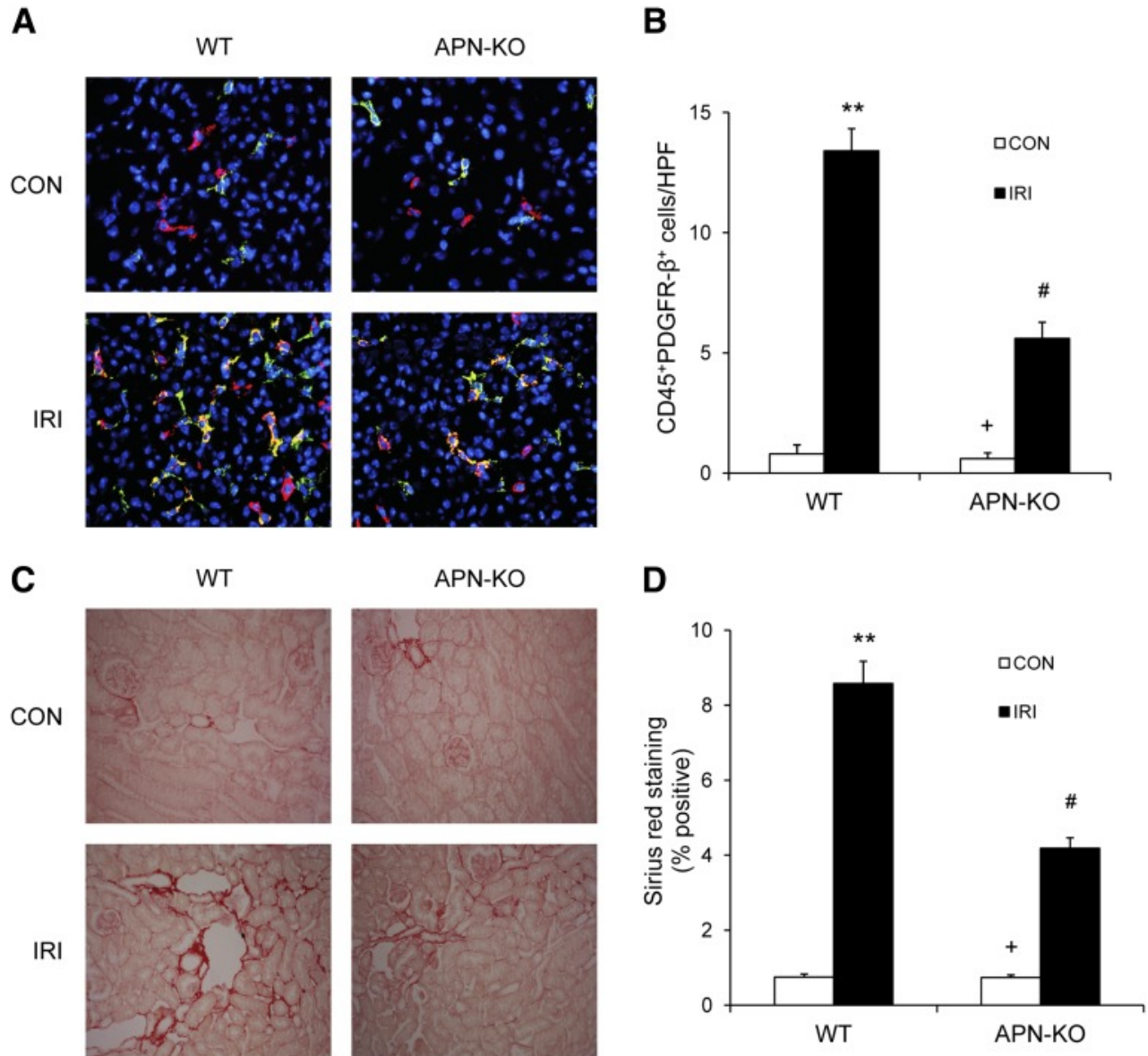
Adiponectin deficiency reduces myeloid fibroblast accumulation and renal fibrosis after ischemia/reperfusion injury (IRI). (A) Representative photomicrographs of kidney sections from WT and adiponectin KO mice 7 days after ischemia/reperfusion injury stained for CD45 (red), PDGFR-β (green), and DAPI (blue) (original magnification, ×X400). B. Quantitative analysis of CD45$^+$ and PDGFR-β$^+$ fibroblasts in the kidneys of WT and adiponectin KO mice 7 days after ischemia/reperfusion injury. **$P<0.01$ versus WT controls (CON), +$P<0.05$ versus KO ischemia/reperfusion injury, and #$P<0.05$ versus WT ischemia/reperfusion injury. $n=6$ per group. (C) Representative photomicrographs of kidney sections from WT and adiponectin KO mice 2 weeks after ischemia/reperfusion injury stained with Sirius red for assessment of total collagen deposition (original magnification ×400). (D) Quantitative analysis of interstitial collagen content in the kidneys of WT and adiponectin KO mice. **$P<0.01$ versus WT controls, +$P<0.05$ versus KO ischemia/reperfusion injury, and #$P<0.05$ versus WT ischemia/reperfusion injury. $n=6$ per group. APN, adiponectin.
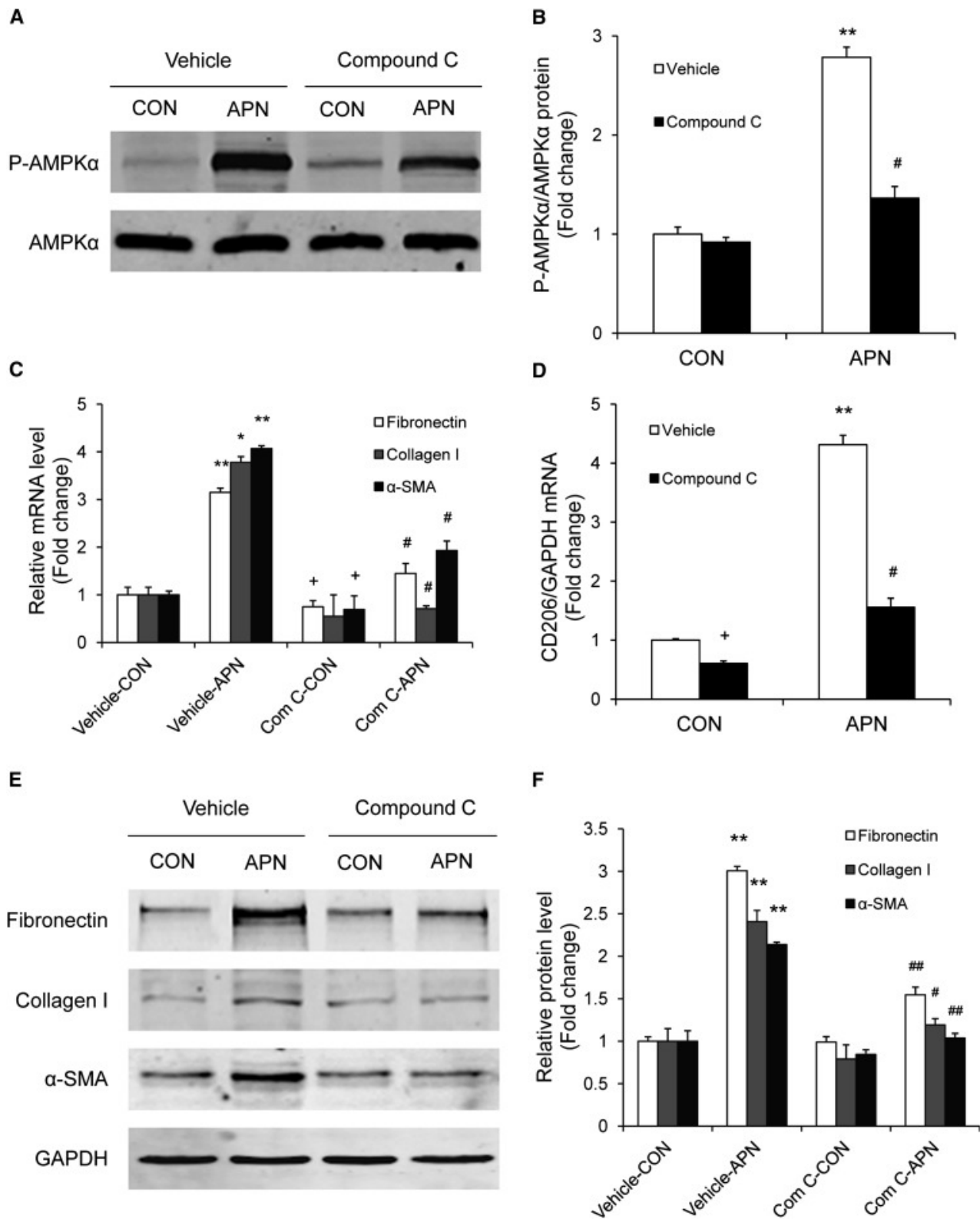
Figure 8.
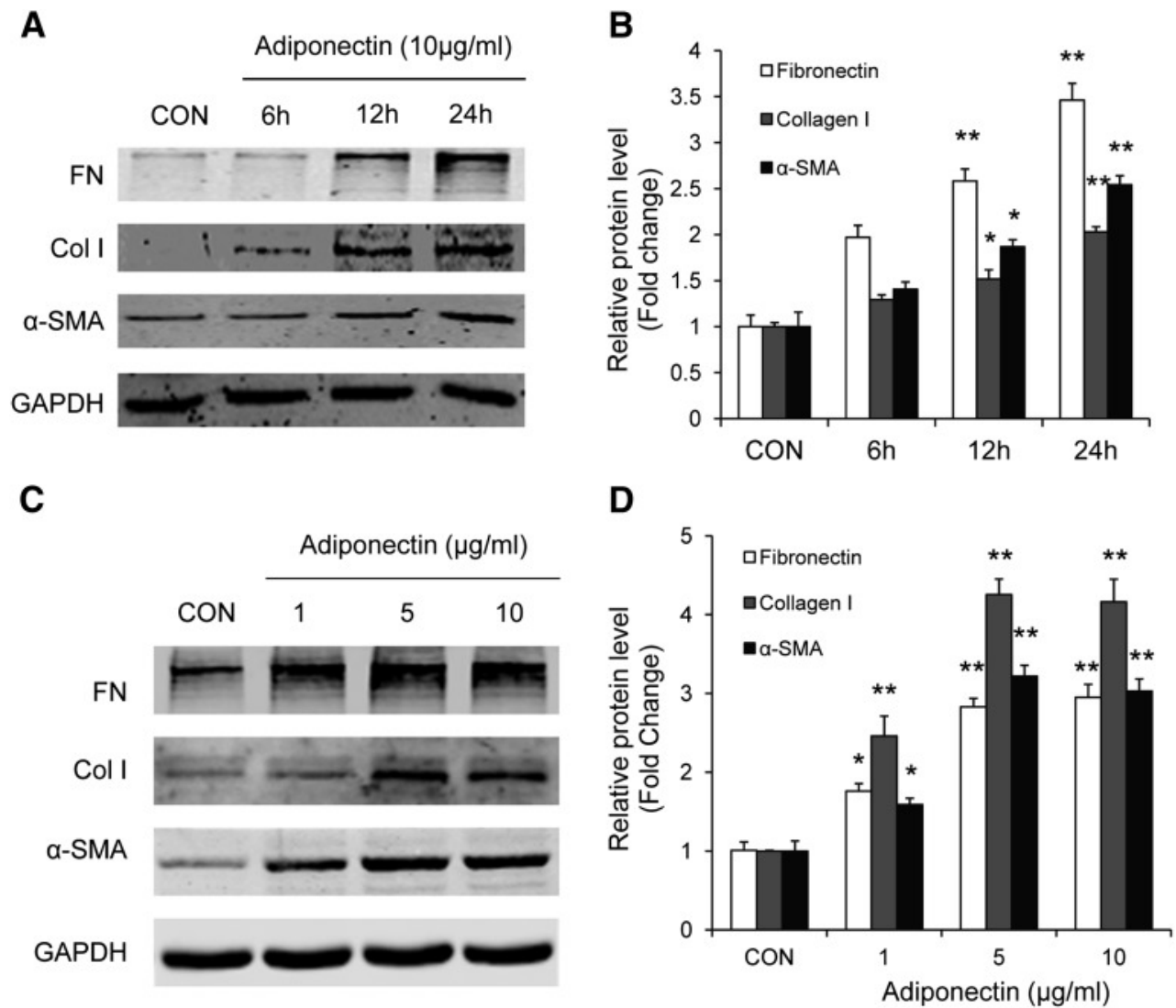
Adiponectin promotes monocyte-to-fibroblast transition and matrix protein production in bone marrow–derived monocytes in a time- and dose-dependent manner. Adiponectin time-dependently increases protein expression of fibronectin, collagen I, and α-SMA in bone marrow–derived monocytes (A and B). Adiponectin time-dependently increases protein expression of fibronectin, collagen I, and α-SMA in bone marrow–derived monocytes (C and D). *$P<0.05$ versus vehicle controls (CON), **$P<0.01$ versus vehicle controls. $n=3$ per group.

Figure 9.
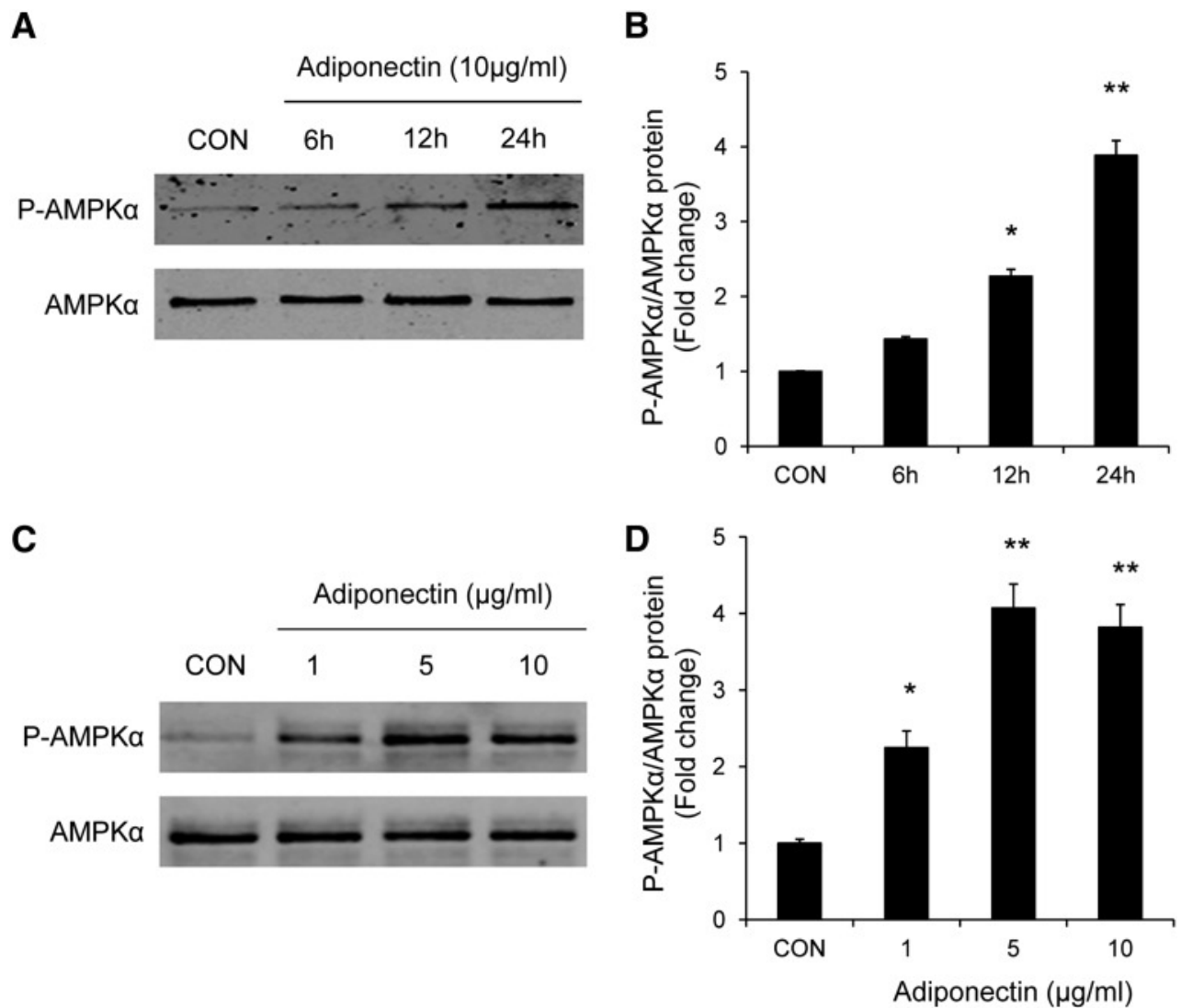
Adiponectin activates AMPK in bone marrow–derived monocytes in a time- and dose-dependent manner. Bone marrow–derived monocytes were incubated for different time periods with various concentrations of adiponectin as indicated. Cell lysates were immunoblotted with indicated antibodies. Adiponectin time-dependently induces phosphorylation of AMPKα in bone marrow–derived monocytes (A and B). Adiponectin dose-dependently induces phosphorylation of AMPKα in bone marrow–derived monocytes (C and D). *$P<0.05$ versus vehicle controls (CON), **$P<0.01$ versus vehicle controls. $n=3$ per group. p-AMPK, phosphorylated-AMPK.
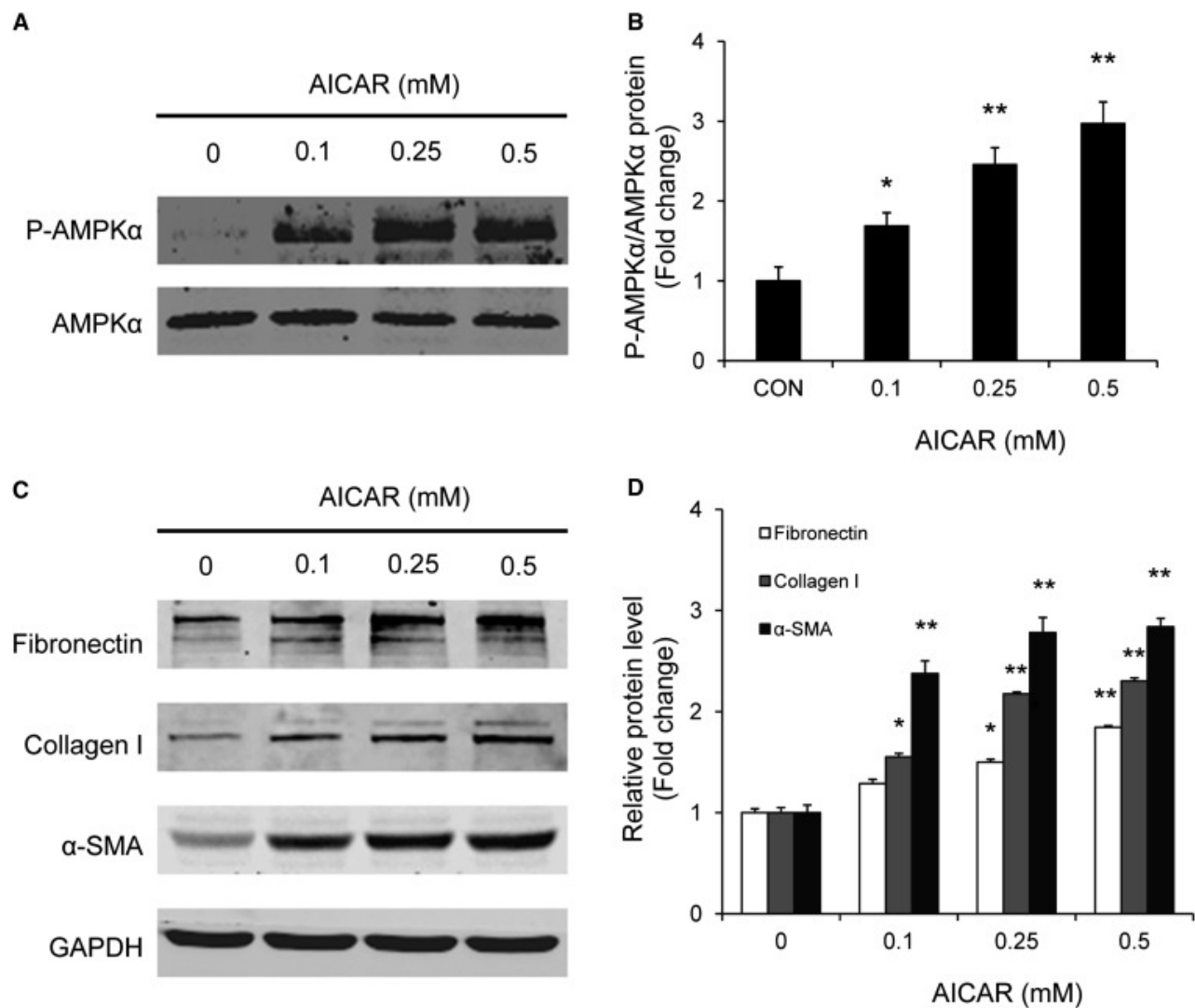
Figure 10.

Compound C blocks adiponectin-induced AMPK activation and monocyte-to-fibroblast transition and matrix protein production in bone marrow–derived monocytes. Bone marrow–derived monocytes were incubated with 10 mg/ml of adiponectin for 24 hours in the absence or presence of 10 μM of compound C. Western blot analysis shows that compound C inhibits adiponectin-induced AMPKα phosphorylation (A and B). Real-time RT-PCR demonstrates that compound C abolishes adiponectin-induced gene expression of fibronectin, collagen I, α-SMA, and CD206 (C and D). Western blot analysis shows that compound C reduces adiponectin-induced protein expression of fibronectin, collagen I, and α-SMA (E and F). *$P<0.05$ versus vehicle controls (CON); **$P<0.01$ versus vehicle controls; [#]$P<0.05$ versus APN; [##]$P<0.01$ versus APN. $n=3$ per group. APN, adiponectin.

Figure 11.

A

Ad-GFP   Ad-DN-AMPKα1

CON   APN   CON   APN

HA

GAPDH

P-AMPKα

AMPKα

B
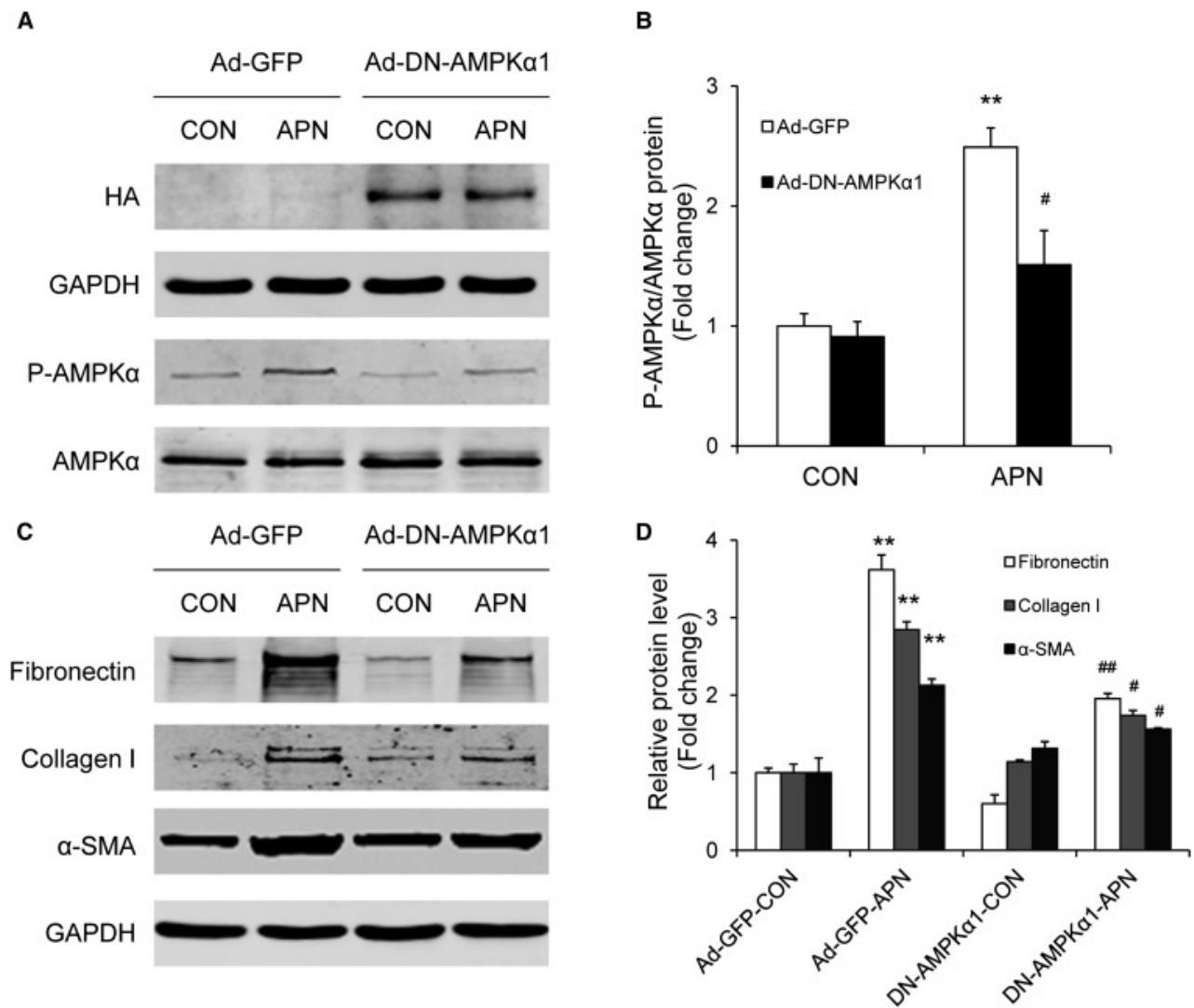
Expression of a dominant negative AMPK prevents adiponectin-induced monocyte-to-fibroblast transition and matrix protein production in bone marrow–derived monocytes. Bone marrow–derived monocytes were transduced with Ad-DN-AMPKα or Ad-GFP (as a control [CON]) at a multiplicity of infection of 100 for 48 hours and then were incubated with adiponectin or vehicle for 24 hours. Cell lysates were immunoblotted with specific antibodies as indicated. **$P<0.01$ versus Ad-GFP controls; #$P<0.05$ versus Ad-GFP-APN; ##$P<0.01$ versus Ad-GFP-APN. $n=3$ per group. p-AMPK, phosphorylated-AMPK.

Figure 12.

AICAR time-dependently activates AMPK and promotes monocyte-to-fibroblast transition and matrix protein production in bone marrow–derived monocytes. Bone marrow–derived monocytes were incubated with AICAR at 0.5 mM or vehicle for different periods of time. Cell lysates were immunoblotted with indicated antibodies. AICAR time-dependently induces phosphorylation of AMPKα (A and B) and increases protein expression of fibronectin, collagen I, and α-SMA (C and D). *$P<0.05$ versus vehicle-treated controls (CON), **$P<0.01$ versus vehicle-treated controls. $n=3$ per group.

Figure 13.

A

B

C

D
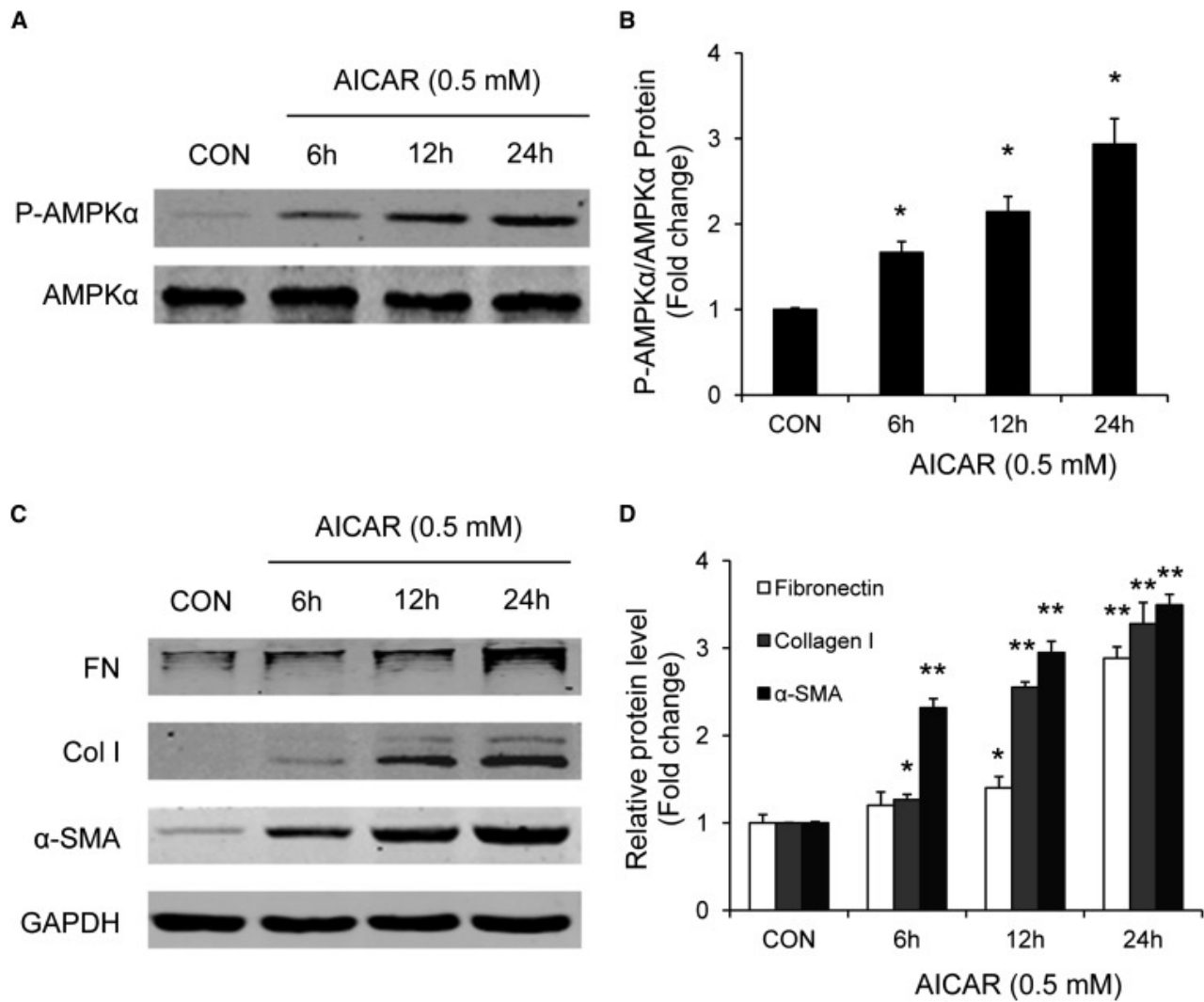
AICAR dose-dependently activates AMPK and promotes monocyte-to-fibroblast transition and matrix protein production in bone marrow–derived monocytes. Bone marrow–derived monocytes were incubated with various doses of AICAR for 24 hours. Cell lysates were immunoblotted with indicated antibodies. AICAR dose-dependently induces phosphorylation of AMPKα (A and B) and increases protein expression of fibronectin (FN), collagen I (Col I), and α-SMA (C and D). *$P<0.05$ versus vehicle-treated controls (CON), **$P<0.01$ versus vehicle-treated controls. $n=3$ per group. p-AMPK, phosphorylated-AMPK.